ORGANIC LETTERS

2011
Vol. 13, No. 22
5960–5963

Thiophene-Fused Tetracene Diimide with Low Band Gap and Ambipolar Behavior

Qun Ye,[†] Jingjing Chang,[†] Kuo-Wei Huang,[‡] and Chunyan Chi*[,†]

Department of Chemistry, National University of Singapore, 3 Science Drive 3, Singapore, 117543, and KAUST Catalysis Center and Division of Chemical and Life Sciences and Engineering, 4700 King Abdullah University of Science and Technology, Thuwal 23955-6900, Kingdom of Saudi Arabia

chmcc@nus.edu.sg

Received August 31, 2011

ABSTRACT

The first tetracene diimide derivative fused with four thiophene rings, TT-TDI, was synthesized by an $FeCl_3$ mediated oxidative cyclodehydrogenation reaction. TT-TDI exhibited a low band gap of 1.52 eV and amphoteric redox behavior. TT-TDI also showed a liquid crystalline property and ambipolar charge transport in thin film field-effect transistors.

Acenes have been intensively investigated for their potential as charge transporting materials.[1] However, their practical applications are usually limited by relatively poor chemical and photostability.[2] Various methods have been applied to improve their stability which include (1) substitution by aryl, silylethyne, or thioether groups and (2) fluorination and substitution with fluorinated groups.[2] Alternatively, attachment of electron-withdrawing dicarboximide groups is supposed to be an efficient way to lower the HOMO energy level of acenes and thus to improve their stability. Our group recently prepared a series of stable pentacene diimide derivatives by lateral substitution with dicarboximide groups.[3] Since the most reactive sites of acenes are located at the zig-zag edges, vertical attachment of dicarboximide groups is believed to be more efficient to obtain highly stable acene imides. So far, only naphthalene mono- or diimides,[4] anthracene mono- and diimide,[5] and tetracene monoimides[6] with the imide group attached onto the zig-zag edges have been reported. Synthesis of longer acenes substituted by more than one vertically attached imide group is challenging. Herein, we report the first successful synthesis of a tetrathienyl-fused tetracene diimide **TT-TDI** (Scheme 1). Our strategy is to make a core expansion from a smaller naphthalene diimide building block such as **1** (Scheme 1), and the obtained compound **TT-TDI** is expected to show a low band gap and long wavelength absorption due to intramolecular donor−acceptor interaction.

[†] National University of Singapore.
[‡] King Abdullah University of Science and Technology.

(1) (a) Bendikov, M.; Wudl, F.; Perepichka, D. F. *Chem. Rev.* **2004**, *104*, 4891. (b) Anthony, J. E. *Chem. Rev.* **2006**, *106*, 5028. (c) Anthony, J. E. *Angew. Chem., Int. Ed.* **2008**, *47*, 452. (d) Sánchez-Carrera, R. S.; Paramonov, P.; Day, G. M.; Coropceanu, V.; Brédas, J.-L. *J. Am. Chem. Soc.* **2010**, *132*, 14437.

(2) (a) Parne, M. M.; Parkin, S. R.; Anthony, J. E. *J. Am. Chem. Soc.* **2005**, *127*, 8028. (b) Kaur, I.; Jia, W.; Kopreski, R. P.; Selvarasah, S.; Dokmeci, M. R.; Pramanik, C.; McGruer, N. E.; Miller, G. P. *J. Am. Chem. Soc.* **2008**, *130*, 16274. (c) Chun, D.; Cheng, Y.; Wudl, F. *Angew. Chem., Int. Ed.* **2008**, *47*, 8380. (d) Qu, H.; Chi, C. *Org. Lett.* **2010**, *12*, 3360. (e) Kaur, I.; Jazdzyk, M.; Stein, N. N.; Prusevich, P.; Miller, G. P. *J. Am. Soc. Chem.* **2010**, *132*, 1261. (f) Purushothaman, B.; Bruzek, M.; Parkin, S. R.; Miller, A.-F.; Anthony, J. E. *Angew. Chem., Int. Ed.* **2011**, *50*, 7013.

(3) Qu, H.; Cui, W.; Li, J.; Shao, J.; Chi, C. *Org. Lett.* **2011**, *13*, 924.

(4) (a) Katz, H. E.; Lovinger, A. J.; Johnson, J.; Kloc, C.; Siegrist, T.; Li, W.; Lin, Y.-Y.; Dodabalapur, A. *Nature* **2000**, *404*, 478. (b) Jones, B. A.; Facchetti, A.; Marks, T. J.; Wasielewski, M. R. *Chem. Mater.* **2007**, *19*, 2703. (c) Gao, X.; Di, C.-A.; Hu, Y.; Yang, X.; Fan, H.; Zhang, F.; Liu, Y.; Li, H.; Zhu, D. *J. Am. Chem. Soc.* **2010**, *132*, 3697. (d) Hu, Y.; Gao, X.; Di, C. -A.; Yang, Y.; Zhang, F.; Liu, Y.; Li, H.; Zhu, D. *Chem. Mater.* **2011**, *23*, 1204.

(5) (a) Yao, J.; Chi., C.; Wu, J.; Loh, K. *Chem.—Eur. J.* **2009**, *15*, 9299. (b) Mohebbi, A. R.; Munoz, C.; Wudl, F. *Org. Lett.* **2011**, *13*, 2560.

(6) Yin, J.; Zhang, K.; Jiao, C.; Li, J.; Chi, C.; Wu, J. *Tetrahedron Lett.* **2010**, *51*, 6313.

10.1021/ol202357f
Published on Web 10/14/2011

Scheme 1. Synthetic Route of **TT-TDI** and Related Precursors

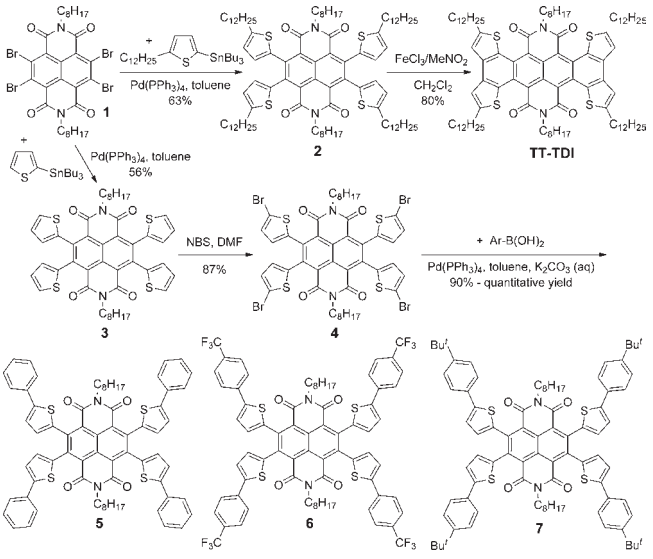

TT-TDI is also designed to have a rigid core attached with flexible alkyl chains so that it can show liquid crystalline properties. Application of **TT-TDI** in thin-film field-effect transistors was also investigated.

Synthesis of **TT-TDI** and related precursors is shown in Scheme 1. The starting material 2,3,6,7-tetrabromo naphthalene diimide **1** was synthesized according to reported literature.[7] Tetrathienyl-substituted naphthalene diimide **2** was prepared by a 4-fold Stille coupling of **1** with tributyl(5-dodecylthiophen-2-yl)stannane.[8] It is worthy to note that the catalyst loading of this 4-fold Stille coupling reaction had to be carefully controlled in order to avoid any phosphonium salt formation.[9] By lowering the loading of $Pd(PPh_3)_4$ to 0.03 equiv per bromine, the target product **2** was obtained in a 63% yield. Subsequent ferric chloride mediated oxidative cyclization[10] of **2** successfully gave the final product **TT-TDI** in 80% yield. Such intramolecular cyclization was thought to be challenging because (1) the electron-deficient naphthalene diimide core will increase the oxidation potential which makes the oxidative cyclization hard to occur and (2) there is significant steric repulsion between the thiophene units and the carbonyl group, which gives extra barriers for the reaction to occur.

The success on **TT-TDI** provoked us to further extend this strategy to the synthesis of more tetrathienyl-fused tetracene diimides. Thus, precursors **5**, **6**, and **7** with different substituents were prepared (Scheme 1). Compound **1** underwent similar 4-fold Stille coupling reactions to give the tetrathiophene-substituted naphthalene diimide **3** in 56% yield. Bromination of **3** with NBS in DMF[11] afforded **4** in 87% yield, and subsequent 4-fold Suzuki coupling reactions provided compounds **5**–**7** in good yields. Precursors **5**–**7** were then submitted for ferric chloride mediated oxidative cyclodehydrogenation. However, reaction of **5** generated a dark blue mixture which contained intermolecular coupling products and chlorinated side products based on mass spectrometry analysis. By lowering the oxidant loading or decreasing the reaction temperature from room temperature to 0 °C, this problem was not well resolved. We reasoned that the *para*-position of the end-capping phenylene ring should be responsible for the undesired reactivity of this precursor. Therefore, in **6** and **7**, the *para*-positions of the phenylene ring are blocked by an electron-withdrawing trifluoromethyl group or electron-donating *tert*-butyl group. For both **6** and **7**, the oxidative cyclization by ferric chloride, however, only generated one-side closed (i.e., −2H) products which were contaminated with starting material and some chlorinated side products, and separation of the mixture was not successful. Prolongation of the reaction time or addition of extra oxidant did not lead to fully cyclized products but more chlorinated side products. To address this problem, we further attempted the cyclization of **4** with the attempt to synthesize a general functionalizable tetracenediimide building block. Again, cyclization of **4** with either ferric chloride or VOF_3/BF_3•Et_2O only gave partially cyclized product together with some chlorinated side products.

To better understand the ring closure reaction, the electrochemical properties of **2** and **4**–**7** were studied by cyclic voltammetry (Figure S1 and Table S1 in the Supporting Information (SI)). All five compounds showed two reversible reduction waves and one irreversible oxidation wave. The successful substrate **2** was found to have a HOMO energy level of −5.73 eV. By changing the dodecyl chain to an electron-deficient bromine and trifluomethyl phenyl group, the HOMO energy levels of **4** and **6** were decreased to −5.99 and −5.85 eV, respectively, and this HOMO energy level decrease would be responsible for their unsuccessful oxidative cyclization. For **5** and **7**, the HOMO energy level increased to −5.67 and −5.59 eV, respectively. With the substituents being electron-rich, the radical cation generated might delocalize along the thienyl-phenyl unit and this may lead to unwanted intermolecular coupling, chlorination, and low reactivity of the cation. Therefore, the oxidation potential of the precursor played a key role on the oxidative cyclization reaction.

In solution, both **2** and **TT-TDI** exhibited a strong π–π^* transition with a maximum absorption at *ca.* 370 nm and a strong charge transfer band at 494 and 655 nm,

(7) Gao, X.; Qiu, W.; Yang, X.; Liu, Y.; Wang, Y.; Zhang, H.; Qi, T.; Liu, Y.; Lu, K.; Du, C.; Shuai, Z.; Yu, G.; Zhu, D. *Org. Lett.* **2007**, *9*, 3917.

(8) Luo, J.; Huang, K.; Qu, H.; Zhang, X.; Zhu, L.; Chan, H.; Chi, C. *Org. Lett.* **2010**, *12*, 5660.

(9) (a) The generated high polar byproduct has red color and good solubility in chloroform if the catalyst loading is greater than 0.03 equiv per bromine. MS and ^{1}H NMR results indicate that one triphenylphosphine is attached to the core with the loss of one bromine atom. (b) Melpoder, J. B.; Heck, R. F. *J. Org. Chem.* **1976**, *41*, 265. (c) Ziegler, C. B.; Heck, R. F. *J. Org. Chem.* **1978**, *43*, 2941. (d) Marcoux, D.; Charette, A. B. *J. Org. Chem.* **2008**, *73*, 590.

(10) Wu, J.; Pisula, W.; Müllen, K. *Chem. Rev.* **2007**, *107*, 718.

(11) Krüger, H.; Janietz, S.; Sainova, D.; Dobreva, D.; Koch, N.; Vollmer, A. *Adv. Funct. Mater.* **2007**, *17*, 3715.

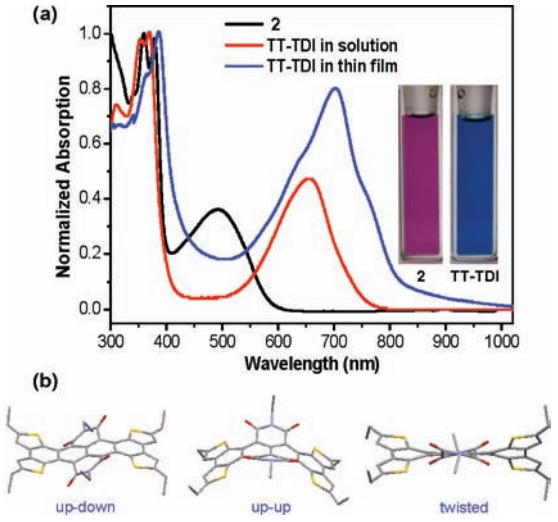

Figure 1. (a) UV−vis absorption spectra of **2** and **TT-TDI** in chloroform solution (1.0×10^{-5} M) and in thin film. Insert: photos for the dilute solution of **2** and **TT-TDI** in chloroform. (b) Calculated three conformers of **TT-TDI**.

respectively (Figure 1a). Accordingly, the solution color of **2** and **TT-TDI** was purple and blue, respectively (Figure 1a). The absorption maximum of the charge transfer peak was red-shifted about 160 nm after ring closure, indicating that **TT-TDI** had a lower band gap and more extended π-system. In the solid state, **TT-TDI** showed a bathochromic shift of 47 nm due to aggregation at the solid state (Figure 1a). The lowest energy absorption onset of the solution absorption was at 754 nm, and the optical band gap was calculated to be 1.64 eV for **TT-TDI**. **TT-TDI** exhibited a very weak emission peak with an emission maximum at *ca.* 775 nm when excited at 650 nm (Figure S2 in SI) due to the charge transfer nature of the molecule.

Time-dependent density function theory (TDDFT at B3LYP/6-31G*) calculations were conducted for **TT-TDI** to understand its electronic and optical properties. Due to steric congestion between the fused thiophene rings and the carbonyl groups, three possible conformers, denoted as up−down, up−up, and twisted, were evaluated (Figure 1b). The up−down conformer has the lowest energy (1.5−3.5 kcal/mol more stable), but all conformers show a similar calculated absorption spectrum with two major bands at 347 nm (HOMO to LUMO + 2) and 627 nm (HOMO−1 to LUMO) (see SI). The band shapes are in good agreement with the experimental data.

TT-TDI exhibited amphoteric redox properties with one reversible 1e oxidation wave with half wave potential $E_{1/2}{}^{ox}$ at 0.94 V (vs Fc^+/Fc), two reversible 1e reduction waves with half wave potential $E_{1/2}{}^{red}$ at −0.77 V and −0.89 V (vs Fc^+/Fc), respectively, and one irreversible reduction wave (Figure 2 and Table S1). A HOMO energy level of −5.62 eV and a LUMO energy level of −4.10 eV were estimated based on the onset potential of the first oxidation wave and the first reduction wave, respectively. The electrochemical

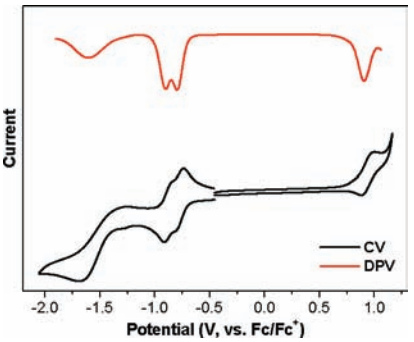

Figure 2. Cyclic voltammogram (CV) and differential pulse voltammogram (DPV) of **TT-TDI** in dry DCM with 0.1 M Bu_4NPF_6 as supporting electrolyte.

energy gap was calculated to be 1.52 eV. It is worth noting that the HOMO of **TT-TDI** only changed slightly compared with **2** while the LUMO decreased from −3.73 eV for **2** to −4.10 eV for **TT-TDI** after cyclization. The low lying LUMO energy level implies that **TT-TDI** can serve as an electron transporting material.

The differential scanning calorimetry (DSC) curve of **TT-TDI** showed two endothermic peaks at 13 and 146 °C upon heating and two exothermic peaks at 2 and 101 °C upon cooling (Figure 3a). From polarizing optical microscope (POM) analysis, **TT-TDI** entered an isotropic phase at 150 °C upon heating, and upon slow cooling from the isotropic phase, a typical texture for a columnar liquid crystalline mesophase was observed until room temperature (insert in Figure 3a). That means **TT-TDI** is actually a room-temperature liquid crystal. A powder XRD pattern of **TT-TDI** recorded at room temperature revealed a series of sharp reflection peaks which can be correlated to the (100), (200), and (300) reflections of a lamellar structure with an interlayer distance of 2.71 nm (Figure 3b). In addition, a reflection peak at 4.48 Å was also observed, which can be correlated to the long-range ordered π-stacking between the rigid but nonplanar core.

Field-effect transistors were fabricated by spin-coating the solution of **TT-TDI** in chloroform onto an octadecyltrimethoxysilane (OTMS) modified SiO_2/Si substrate in a top-contact configuration (gold as source/drain electrodes). The devices were annealed at 90 °C under nitrogen. Devices based on **TT-TDI** mainly exhibited n-type behavior when measured under nitrogen (Figure 4a−b), with an average saturation electron mobility $\mu_{sat}(e) = 4.83 \times 10^{-3}$ $cm^2/(V\ s)$, threshold voltage $V_{th} = 56$ V, and On/Off ratio $= 5 \times 10^5$. However, in air, the device exhibited typical ambipolar character (Figure 4c−d), with $\mu_{sat}(e) = 7.4 \times 10^{-4}$ $cm^2/(V\ s)$, $V_{th} = 40$ V, and On/Off ratio $= 10^3$−10^4 for *n*-channel operation and $\mu_{sat}(h) = 9.0 \times 10^{-4}$ $cm^2/(V\ s)$, $V_{th} = -20$ V, and On/Off ratio $= 10^3$−10^4 for *p*-channel operation. The hole transport was enhanced in ambient perhaps due to doping by molecular oxygen. Such an ambipolar charge transporting character and the observed amphoteric redox behavior must originate from its

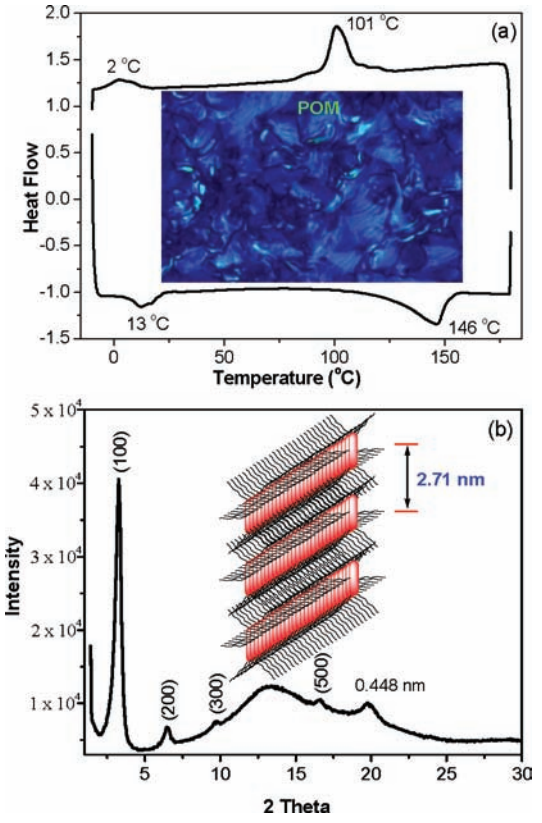

Figure 3. (a) The first cooling and the second heating DSC curves of **TT-TDI** measured under a nitrogen atmosphere with heating/cooling rate of 10 °C/min. Insert is the polarizing optical microscope image recorded at 136 °C during cooling. (b) Powder XRD pattern of **TT-TDI** recorded at 30 °C. Insert is the proposed layer-like packing mode.

small band gap. Atomic force microscope (AFM) measurements showed a highly ordered liquid crystalline thin film after thermal annealing, which is in accordance with the XRD results. The thin-film XRD pattern indicated an ordered packing with up to five orders of diffraction. And the out of plane *d*-spacing of 2.71 nm in thin film corresponds to the interlayer distance which suggests a layer-like superstructure (see SI).

In summary, we have successfully synthesized the first tetracene diimide **TT-TDI** fused with four electron-rich thiophene units. It was found that the HOMO energy level of the precursors is crucial for successful oxidative cyclization mediated by ferric chloride. **TT-TDI** has a small band

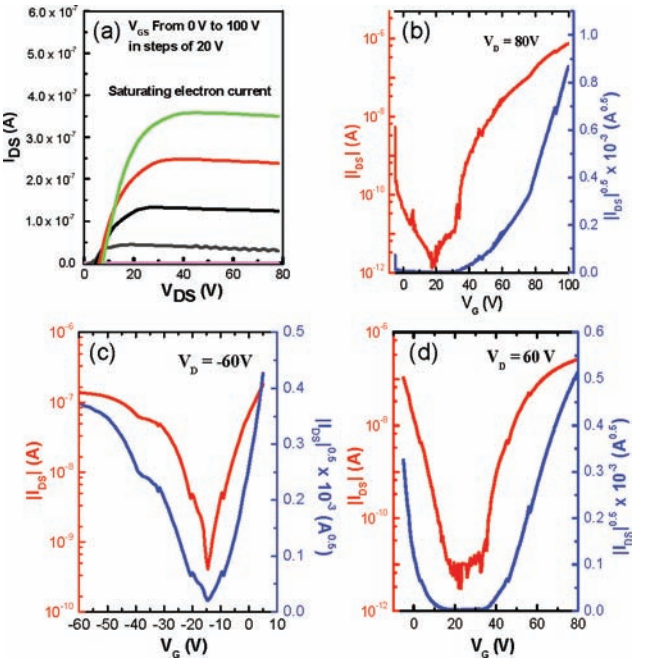

Figure 4. Output (a) and transfer (b–d) characteristic of the OFETs based on **TT-TDI**. (a–b) Measured under nitrogen; (c–d) measured in air.

gap due to intramolecular donor–acceptor interaction as well as extended π-conjugation, and it displays amphoteric redox behavior. It is worth noting that, although with a nonplanar core structure, the **TT-TDI** showed ordered self-assembly and exhibited room-temperature liquid crystalline properties. Ambipolar charge transport was also observed in thin film field-effect transistors.

Acknowledgment. C.C. acknowledges financial support from the National University of Singapore under MOE AcRF FRC Grants R-143-000-444-112 and Start Up Grant R-143-000-486-133. K.-W.H. acknowledges the financial support from KAUST.

Supporting Information Available. Synthetic procedures and characterization data for all new compounds, PL spectrum of **TT-TDI**, additional CV data, theoretical calculation details, and more data on device fabrication and characterization. This material is available free of charge via the Internet at http://pubs.acs.org.